Peripheral Vascular Impedance Plethysmography for Respiratory Rate Estimation using Beat-to-Beat Features

Michael Klum¹, Dennis Osterland¹, Alexandu-Gabriel Pielmus¹, Timo Tigges¹, Reinhold Orglmeister¹

Technische Universität Berlin, Chair of Electronics and Medical Signal Processing, Einsteinufer 17, Berlin, Germany

Contact: michael.klum@tu-berlin.de

Abstract

The importance of reduced obtrusion when monitoring bio-parameters is increasing. For acquiring the respiratory rate comfortably at the peripherals, the reflectance photoplethysmogram has been proposed. In some cases, however, even highly integrated, optical measurements are too bulky. Using textile integrated electrodes, for example in socks or gloves, respiratory rate estimation in a low-complexity and minimally obtrusive, wearable scenario might be possible using impedance measurements. We propose using the vascular impedance plethysmography combined with computationally lightweight respiratory rate estimation. Using time-domain beat-to-beat features followed by a spectral feature fusion step we show the feasibility of this concept. We identify suitable feature combinations from seven time-domain features and achieve accuracies beyond 90% with a mean absolute error of 1.7±3.3 breaths per minute. The derived surrogate respiratory signals contain additional information which could be used for more advanced analysis. We conclude that vascular impedance plethysmography is a suitable approach for respiratory rate estimation in minimally obtrusive scenarios.

Introduction

Unobtrusive monitoring of bio-parameters is gaining importance not only in home-care applications but also in the clinical routine. In addition, the current wave of fitness trackers, health apps and activity monitors show the strongly increasing interest to be well informed about the body's status. In the scientific community, especially the estimation of the respiratory rate (RR) has gained much attention over the last years due to the increased interest in sleep health. In most cases, the electrocardiogram (ECG), photoplethysmogram (PPG) or a combination of both is used to estimate respiratory waveforms and rates [1]. Reflective PPG sensors are widely used in modern fitness trackers and we previously showed that ECG electrode distances as low as 24 mm can still be used to accurately estimate respiratory signals [2]. However, there are cases where these techniques are still too obtrusive. Especially in the context of intense physical activity, circulation disorders and mental illnesses, surface electrodes as used for ECG or wristbands can be too bulky.

One solution are impedance plethysmographic signals derived from the peripheral vascular system [3]. When combined with fiber-based, textile electrodes [4], integrated for example in socks or gloves, they result in a highly unobtrusive respiratory measurement situation.

In this work, we extend the use of the vascular impedance plethysmography (vIPG) in the context of unobtrusive, wearable monitors. We identify suitable, computationally feasible beat-to-beat feature combinations for the RR estimation and propose a feature fusion concept. With our work we hope to lay the groundwork for less obstructive, peripheral RR estimation in a wearable scenario.

Materials and Methods

vIPG Signals and Fiducial Points

Vascular impedance plethysmography signals are obtained using a tetrapolar Ag/AgCl disposable electrode configuration with a spacing of 10 cm on the left arm. The resulting impedance changes, caused by the vascular blood flow, are in the order of tens of milliohm and represent changes in blood volume [5]. We used a measurement frequency of 100 kHz with a current of 900 A.

Due to their plethysmographic nature, the morphology of vIPG signals differs only slightly from the morphology of PPG signals. Therefore, the fiducial points established in PPG signal analysis also apply for vIPG signals. The three points used throughout this paper, namely the onset, systolic peak and diastolic peak, are given in Figure 1 with their respective amplitudes and positions in the pulse. The baseline of a single pulse is defined in this paper as the first degree polynomial interpolation between two consecutive onsets.

For detection of the vIPG onsets, an open-source algorithm for arterial blood pressure signals proposed by Zong et al. was used [6]. The systolic peak is then defined as the extremum between two consecutive onsets. The diastolic peak is found by identifying the minimum of the second derivate of the pulse following the systolic peak, thus the point where the first derivate is closest to zero in a falling slope [7].

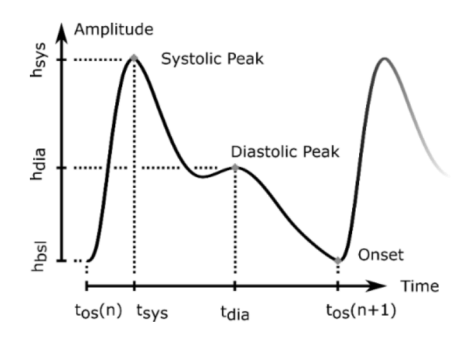


Figure 1: Fiducial points in the plethysmographic signal.



Data Acquisition and Pre-Processing

We measured the vIPG in 10 healthy subjects (6 male, 4 female) aged 26.5 +/- 3.3 years with no prior medical record. For a respiratory reference, pneumotachometer (PNT) signals have been recorded simultaneously. To simulate a short-load situation, a 12 minute long exercise with a four-minute rest, followed by a one-minute load and a seven-minute recovery period was performed using an ergometer. All signals are recorded with 500 samples/s.

The recorded vIPG signal was low-pass filtered with a cutoff frequency of 35 Hz. The baseline-wandering and offset was removed by subtracting a 2000 point gliding mean (GMF). Finally, a 60 point GMF was used to smooth the vIPG signal. The respiratory signal was low-pass filtered at 1 Hz and smoothed using a 150 point GMF.

After pre-processing, the vIPG signals are divided into 20s long signal frames. The quality of each frame is then assessed using an automated procedure based on [8]. If the quality is found to be too low, the frame is rejected.

Beat-to-Beat Features and Reference-Rate

In order to reduce the computational complexity in a low-power embedded environment, we choose seven time-domain features to estimate the respiratory signal [9]. All features as well as their positions within the pulse curve are visualized in Figure 2.

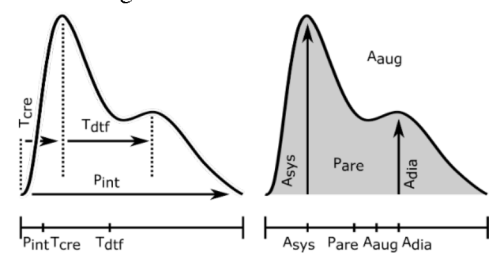


Figure 2: Features and their positions in the pulse curve: left - time based, right - amplitude based.

Each individual pulse, defined as the curve between two onsets, were analyzed separately. First, the pulse onsets of a 20 s interval were found. Next, the individual pulse baseline was removed by subtracting a linear term calculated from the current and next pulse onsets. Then, the two remaining fiducial points were calculated. From the three fiducial points, the seven time domain features given in Table 1 are calculated for each pulse in the frame. In Table 1, the name, symbol as well as the number for each feature is given. The latter is used as an identifier throughout this paper. In addition, the calculation of the feature values and their positions within the current pulse n are defined.

Every feature was assigned a specific time within the pulse, thus spreading the features over the pulse duration as shown in Figure 2. By using specific, feature-dependent times instead of a single position per pulse for all features, a more even distribution of points over the pulse interval is achieved. Thus, the temporal resolution of the estimation is increased when multiple feature vectors are fused. All feature vectors were up-sampled to the original vIPG sample

rate using computationally lightweight piecewise linear interpolation and normalized using the z-score.

The reference RR is calculated from the PNT data by calculating the frequency spectrum using an FFT algorithm. The frequency of the absolute amplitude maximum in the physiologically plausible range of 6 to 36 bpm is considered the reference rate.

Table 1: Time domain beat-to-beat features used.

Nr.	Names	Sym.	Calculation	Time in pulse n	
1	Systolic Am- plitude	A _{sys}	$h_{sys}-h_{bsl} \\$	$t_{os}(n) + t_{sys}$	
2	Diastolic Amplitude	A_{dia}	$h_{dia}-h_{bsl}$	$t_{os}(n) + t_{dia}$	
3	Augmenta- tion Index	A _{aug}	$rac{h_{dia}}{h_{sys}}$	$t_{os}(n) + \frac{t_{dia} - t_{sys}}{2}$	
4	Pulse Area	P _{are}	$\int (Pulse$ $- h_{bsl}) dt$	$t_{os}(n) + \frac{t_{os}(n+1) - t_{os}(n)}{2}$	
5	Pulse Inter- val	P _{int}	$t_{os}(n+1) - t_{os}(n)$	$t_{os}(n)$	
6	Crest Time	T _{cre}	$t_{sys}-t_{os}(n)$	$t_{os}(n) + \frac{t_{sys} - t_{os}(n)}{2}$	
7	Delta-T Feature	T_{dtf}	$t_{dia}-t_{sys}$	$t_{os}(n) + \frac{t_{dia} - t_{sys}}{2}$	

Feature Fusion and Selection

The feature extraction results in seven feature vectors. The following feature fusion is based on three assumptions:

- 1. The respiratory frequency is contained in all feature vectors with an unknown power.
- 2. Unwanted, interfering frequency components are present which may exceed the power of the respiratory frequency.
- 3. The unwanted, interfering frequency components are weakly correlated amongst the feature vectors.

Due to assumptions 1 and 2, extracting the RR by a single feature can prove difficult. Following assumption 3, the performance can be increased if the frequency spectra of the feature vectors are averaged so that the weakly correlated interferences are cancelled out. Due to the property of linearity of the Fourier transform, the normalized signals can be averaged in the time domain and a single FFT of the average signal will suffice, which reduces the computational burden. The peak of the frequency spectrum in the physiologically meaningful interval between 6 and 36 bpm was used as the RR estimation.

In order to optimize the feature selection, we calculated several statistical measures for each possible feature combination and averaged over all 20 s frames. Using the mean absolute error in bpm (MAE_{bpm}) as a performance measure, we ranked the 127 feature combinations to find the combination best suited for the RR estimation.



Statistical Analysis

We used the mean absolute error in bpm (MAE_{bpm}) as the main performance measure to assess the quality of the RR estimation over all 20 s frames. In addition, we calculated the mean error in bmp (ME_{bpm}) to evaluate the systematic bias of the method. By calculating the mean absolute percentage error between the reference RR (RR_{ref}^n) and the estimated RR (RR_{est}^n) over all n 20 s frames we derived the accuracy in percent as given in Equation 1.

$$accuracy = 100 - \frac{100}{n} \sum_{1}^{n} \left| \frac{RR_{est}^{n} - RR_{ref}^{n}}{RR_{est}^{n}} \right|$$
 (1)

Besides the RR estimation performance, we evaluated the monotonic relation of the surrogate respiratory signal and the respiratory reference using the Spearman rank correlation coefficient r in the 20 s frames. Due to the strong phase dependency of r, we furthermore analyzed a lag-adjusted version r_{adj} for applications where signal phase is less important. To derive r_{adj} we calculated the lag between the reference and surrogate respiratory signal using the maximum of their cross correlation. We then shifted the signals accordingly and truncated them to the same length. We then calculated Spearman rank correlation coefficient between these signals which yields r_{adj} .

Results

We first analyzed the seven individual features regarding their single RR estimation performance. The results are given in Table 2, sorted with the best performing feature at the top. Feature 5 (the pulse interval) outperforms all other single features with regard to MAE, correlation and accuracy. The lag-adjusted correlation exceeded 0.7. However, several features achieve a lower bias.

Table 2: Single features sorted based on lowest MAE.

Nr.	MAE _{bpm}	ME_{bpm}	r	r_{adj}	Accuracy
5	2.5±4.1	-2.2±4.3	0.31±0.24	0.70±0.18	84±23%
7	3.5±4.0	-1.9±5.0	0.23±0.16	0.61±0.19	78±23%
1	4.4±5.0	0.3±6.7	0.20±0.16	0.57±0.18	72±33%
4	5.3±5.5	-0.3±7.7	0.22±0.17	0.56±0.18	64±39%
6	5.8±4.4	-2.9±6.7	0.17±0.14	0.53±0.21	63±32%
2	5.9±5.0	-1.8±7.6	0.22±0.18	0.54±0.14	62±34%
3	5.8±5.2	-1.2±7.7	0.24±0.16	0.55±0.18	57±50%

Using the proposed spectral fusion step, we analyzed the performance of all 127 possible feature combinations. The three best performing combinations are given in Table 4. The combination 1,5,7 (systolic amplitude, pulse interval, delta-t feature) achieve the best result in MAE; ME and accuracy. Compared to the best single feature 5, the MAE as well as its standard deviation decreased about 0.8 bpm, the

ME and its standard deviation about 0.9 bpm and the accuracy increased about 6 % while lowering the standard deviation by about the same value. The lag-adjusted correlation did not change significantly.

Table 4: Three best performing feature combinations.

Nr.	MAE _{bpm}	ME _{bpm}	r	r_{adj}	Accuracy
1,5,7	1.7±3.3	-1.3±3.5	0.26±0.21	0.68±0.15	90±17%
4,5,7	2.2±3.8	-1.9±4.0	0.29±0.21	0.67±0.16	87±20%
5,7	2.2±3.9	-1.8±4.1	0.29±0.21	0.69±0.16	87±22%

An excerpt of a single 20 s frame is given in Figure 3. In the upper graph, the filtered and normalized vIPG with its fiducial points is displayed. The regular and typical plethysmographic form of the signal is clearly visible. In the central plot, the three single feature vectors 1,5 and 7 and their piecewise linear interpolation are given. On close inspection, the previously mentioned feature-dependent times of the beat-to-beat features are visible. The lower plot shows the reference PNT signal as well as the merged surrogate respiratory signal with its expected phase shift. The effect of the different sampling points of the features within the individual beats is visible.

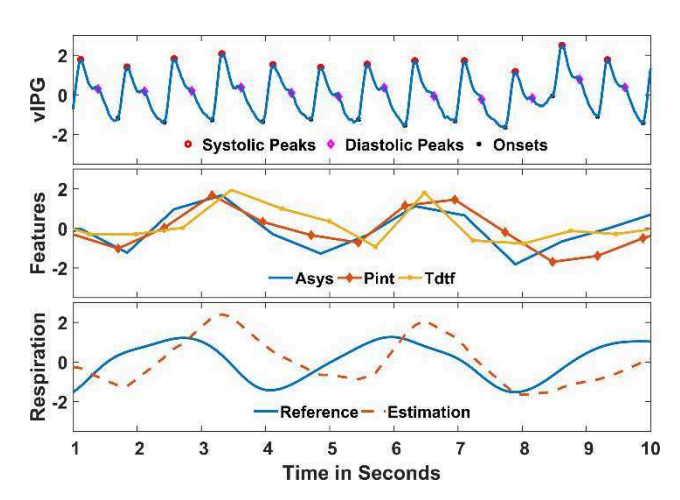


Figure 3: Normalized waveforms of an example frame. Upper – vIPG with fiducial points.

Center – best performing feature vectors.

Bottom – reference respiratory signal and estimation.

In Figure 4 we analyze the RR estimation agreement of the best feature combination 1,5,7 with respect to the reference method using a Bland-Altman diagram. It becomes evident from the plot that about 10 % of the points could be regarded outliers. For the analysis however, we did not remove any outliers as the data was already selected using an automated signal quality estimator. The feature combination does exhibit a slight proportional bias towards the underestimation of lower RR values. Based on visual inspection, the deviation is independent of the absolute value. The negative bias of -1.3 bpm as well as the standard deviation of 3.5 bpm is well explained by the outliers.



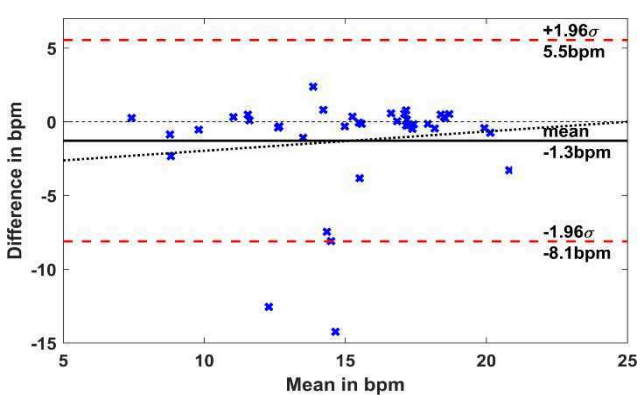


Figure 4: Bland-Altman diagram of the best combination.

Summary

Our aim was to evaluate the use of vascular impedance plethysmography (vIPG) in the peripherals to estimate the respiratory rate (RR). We evaluated 127 combinations of seven time-domain features to find suitable beat-to-beat features for a low-complexity and minimally obstructive RR estimation in a wearable scenario. As the vIPG signal morphology differs only slightly from PPG signals, we are using PPG respiratory rate estimation reports as reference.

We proposed a lightweight spectral feature fusion using linear piecewise interpolation, averaging and FFT to estimate the RR. We found the pulse interval to be the best performing single feature with an MAE of 2.5 bpm and an accuracy of 84%. The best performing feature combination was found to be the systolic amplitude, pulse interval and delta-t feature with an MAE of 1.7 bpm and an accuracy of 90%. The lag-compensated correlation was not affected by the feature fusion and remained at about 0.7 for the best features and combinations. A slight proportional bias towards the underestimation of lower RR values was found.

Discussion

The good performance of the pulse interval feature is most likely due to its close relation to the heart rate and the strong influence from the respiratory sinus arrhythmia.

With respect to reported mean absolute RR estimation errors from the PPG of 1.2 bpm to 10.5 bpm [10], the reported MAE of 1.7 bpm is comparable with the literature. Especially with regard to the lightweight computational approach, the use of the vIPG signal instead of a PPG signal and the relatively short frame length of 20 s, the results are promising. However, a direct comparison with the reported values is difficult due to the different sensors and data used. In addition, we had to reject multiple ill-conditioned frames.

Problems arose from the vastly reduced signal quality in movement and the relatively small signal amplitudes in the range of tens of milliohms. Even though low quality frames were rejected in the signal preprocessing, movement artifacts caused large outliers which in turn degraded the overall statistics. Outliers can be reduced by introducing more rigorous artifact detection than currently implemented. Using guarded electrodes could further increase the signal quality.

The surrogate respiratory signals pose a relatively high lagcompensated rank correlation. They have thus a higher informational content than just the RR. If signal phase is not an issue, this additional information could be used for other purposes, such as the classification of respiratory phases, apnea detection or even classifying pathological breathing. The frame-wise normalization currently limits the possibility for a quantitative assessment of flow or volume parameters.

Conclusion

We conclude that vascular impedance plethysmography is a suitable approach for respiratory rate estimation in minimally obtrusive scenarios. Fusing multiple features can increase the performance to values comparable to state-of-the-art concepts in PPG RR estimation with relatively small computational effort. The surrogate respiratory signals contain additional information which could be used for more advanced analysis. Future work may focus on the integration using textile electrodes, algorithm refining and optimization for other scenarios such as offline processing with higher computational resources.

References

- [1] Charlton, Peter H., et al. An assessment of algorithms to estimate respiratory rate from the electrocardiogram and photoplethysmogram. Physiological measurement, 2016, 37. Jg., Nr. 4, pp. 610.
- [2] Klum, Michael, et al. Minimally spaced electrode positions for multi-functional chest sensors: ECG and respiratory signal estimation. Current Directions in Biomedical Engineering, 2016, 2. Jg., Nr. 1, pp. 695-699.
- [3] Ansari, Sardar, et al. Impedance plethysmography on the arms: Respiration monitoring. In: Bioinformatics and Biomedicine Workshops (BIBMW), 2010 IEEE International Conference on. IEEE, 2010. pp. 471-472.
- [4] Zeng, Wei, et al. Fiber-based wearable electronics: a review of materials, fabrication, devices, and applications. Advanced Materials, 2014, 26. Jg., Nr. 31, pp. 5310-5336.
- [5] Nichols, Wilmer, et al. McDonald's blood flow in arteries: theoretical, experimental and clinical principles. CRC press, 2011.
- [6] Zong, W., et al. An open-source algorithm to detect onset of arterial blood pressure pulses. In: Computers in Cardiology, 2003. IEEE, 2003. pp. 259-262.
- [7] Millasseau, S. C., et al. Determination of age-related increases in large artery stiffness by digital pulse contour analysis. Clinical science, 2002, 103. Jg., Nr. 4, pp. 371-377.
- [8] Orphanidou, Christina, et al. Signal-quality indices for the electrocardiogram and photoplethysmogram: derivation and applications to wireless monitoring. IEEE journal of biomedical and health informatics, 2015, 19. Jg., Nr. 3, pp. 832-838.
- [9] Elgendi, Mohamed. On the analysis of fingertip photoplethysmogram signals. Current cardiology reviews, 2012, 8. Jg., Nr. 1, pp. 14-25.
- [10] Pimentel, Marco AF, et al. Toward a robust estimation of respiratory rate from pulse oximeters. IEEE Transactions on Biomedical Engineering, 2017, 64. Jg., Nr. 8, S. 1914-1923.